Disordered Materials: Glass physics

- 2.7. Introduction, liquids, glasses
- **4.7. Scattering off disordered matter:**
  static, elastic and dynamics structure factors
- 9.7. Static structures:
  X-ray scattering, EXAFS, neutrons, data interpretation
- 11.7. Dynamic structures and the glass transition

HELMHOLTZ GEMEINSCHAFT

Hermann Franz

Methoden moderner Röntgenphysik II
July 2013

DESY

Content

- Systems
- Structure

Dynamics in real disordered solids

- microscopic process: rather harmonic in most glasses

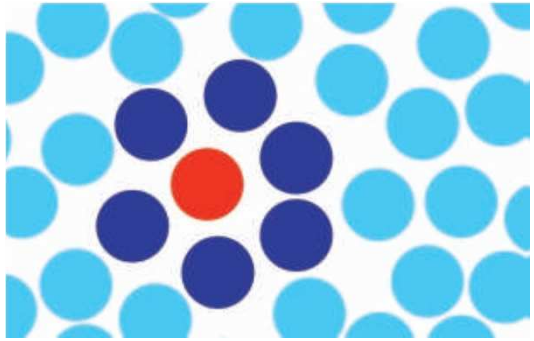

- cage (β)- process: intermediate times

- α- process: long range diffusion, very strong T-dependence, stretched exponential $f_q \exp(-(t/\tau)^{\beta})$

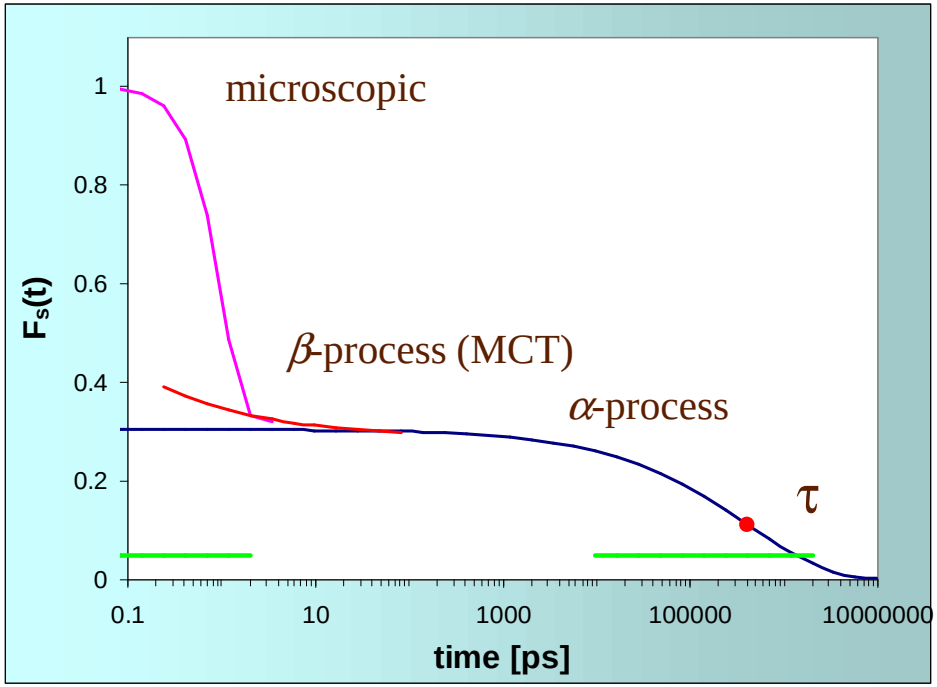

glass transition T_c: α and β process merge

Density correlation functions and MCT

$$\phi_q(t) = \left\langle \rho_q^*(t)\rho_q(0)\right\rangle / \left\langle \left|\rho_q(0)\right|^2 \right\rangle$$

$$\ddot{\phi}_q(t) + \Omega_q^2\phi_q(t) + \Omega_q^2 \int m_q(t-t')\dot{\phi}_q(t')dt' = 0$$

Equation of motion for density correlators including „memory term“

- Ergodicity - non-ergodicity transition at T_c
- Power laws for correlation functions near T_c
- Order parameter is the ergodicity parameter f_q

$$F_q(t) = f_q - h_q(t/\tau)^b + ... \approx f_q \exp(-t/\tau_K)^\beta$$ α-relaxation

$$F_q(t) = f_q + h_q(t_0/t)^a + ...$$ β-relaxation (cage process)

$$f_q \approx \sqrt{T_c - T}$$ Square-root singularity

Density correlation functions and MCT

$$f_q \approx \sqrt{T_c - T}$$

Square-root singularity

T_c describes a transition temperature which in contrast to T_g does not depend on experimental parameters.

The glass transition is an ergodic - non ergodic cross over

In most systems T_c is 20% higher than T_g, i.e. the transition is in the “liquid” region

The glass transition temperature T_g and T_c

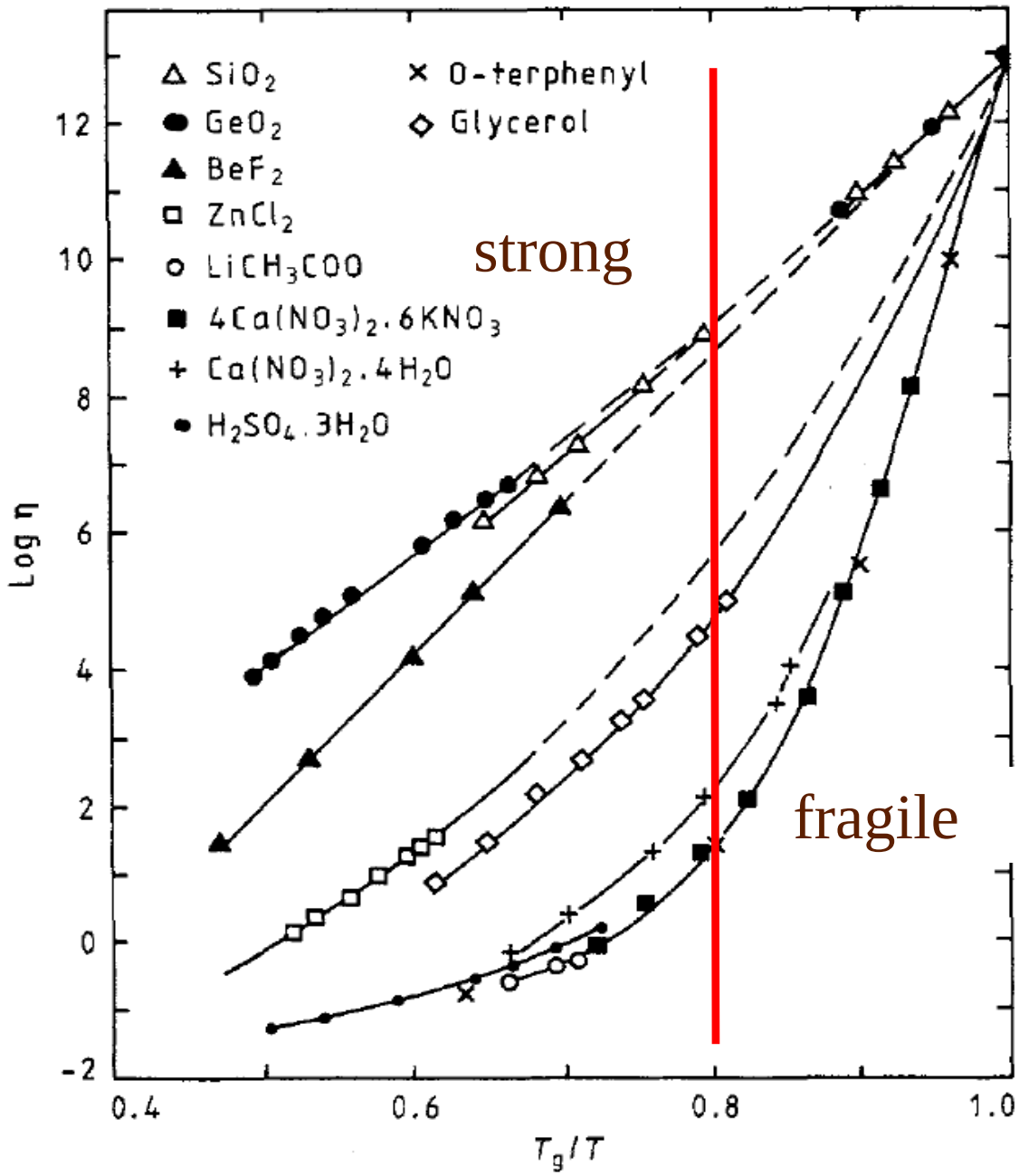

Density correlation functions and MCT

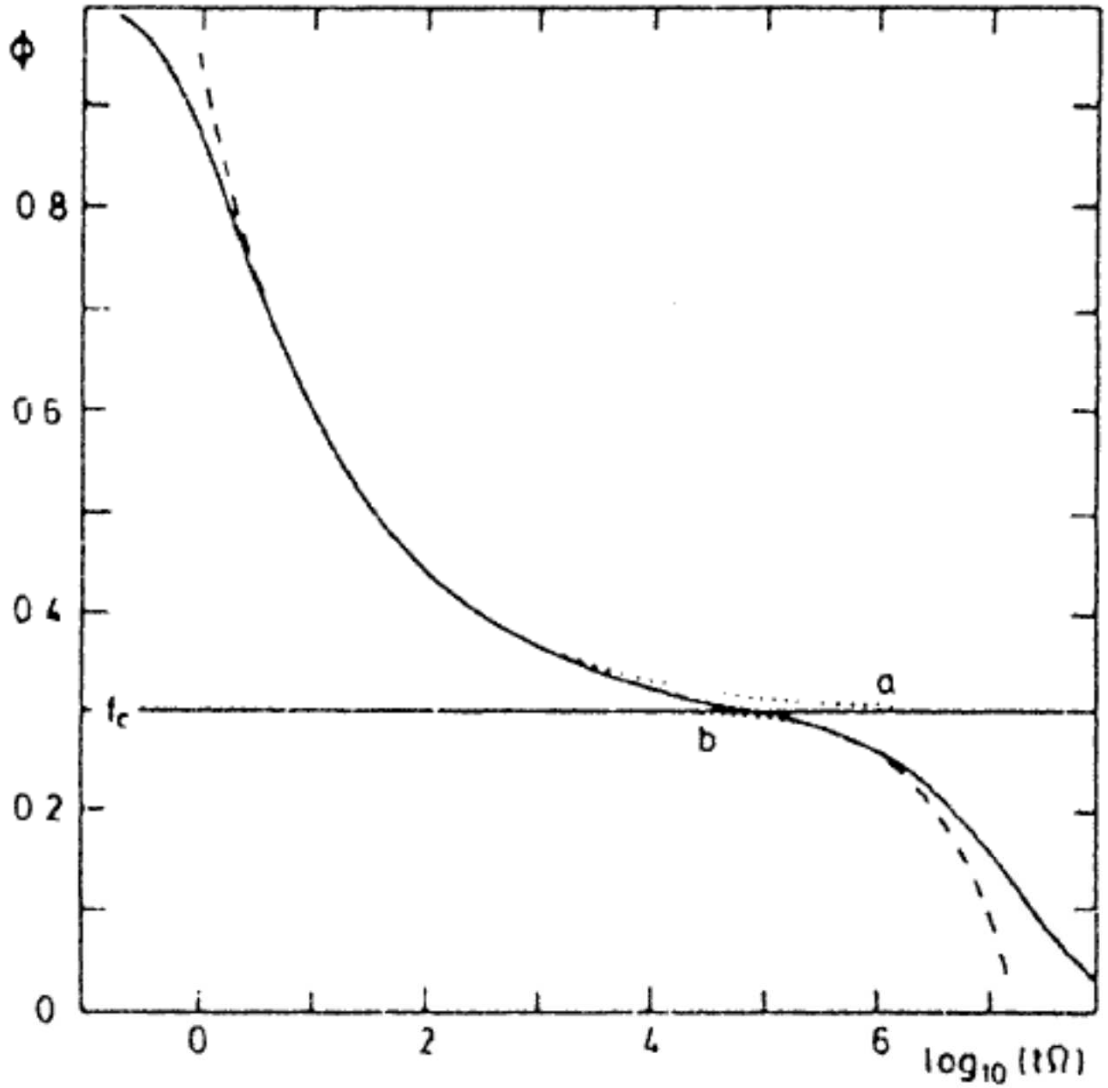

Figure 4. Comparison of the MCT solution for $\phi_q(t)$ (solid curve) with the asymptotic β-relaxation approximation (dashed curve) (equations (25) and (26)). The dotted curves show the two power laws. (From reference [4].)

MCT results for correlation functions at the glass transition

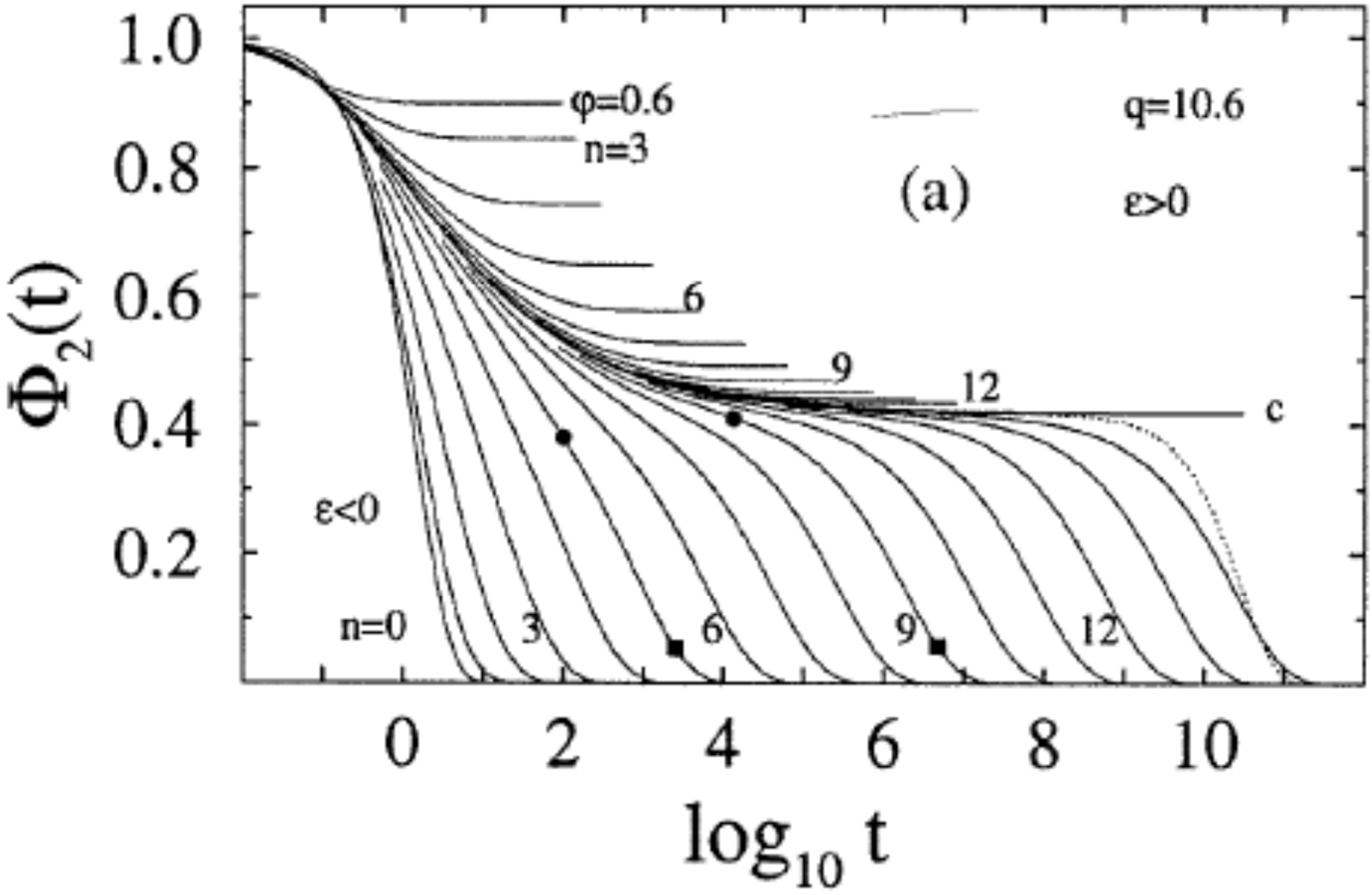

Quasielastic nuclear resonant forward scattering

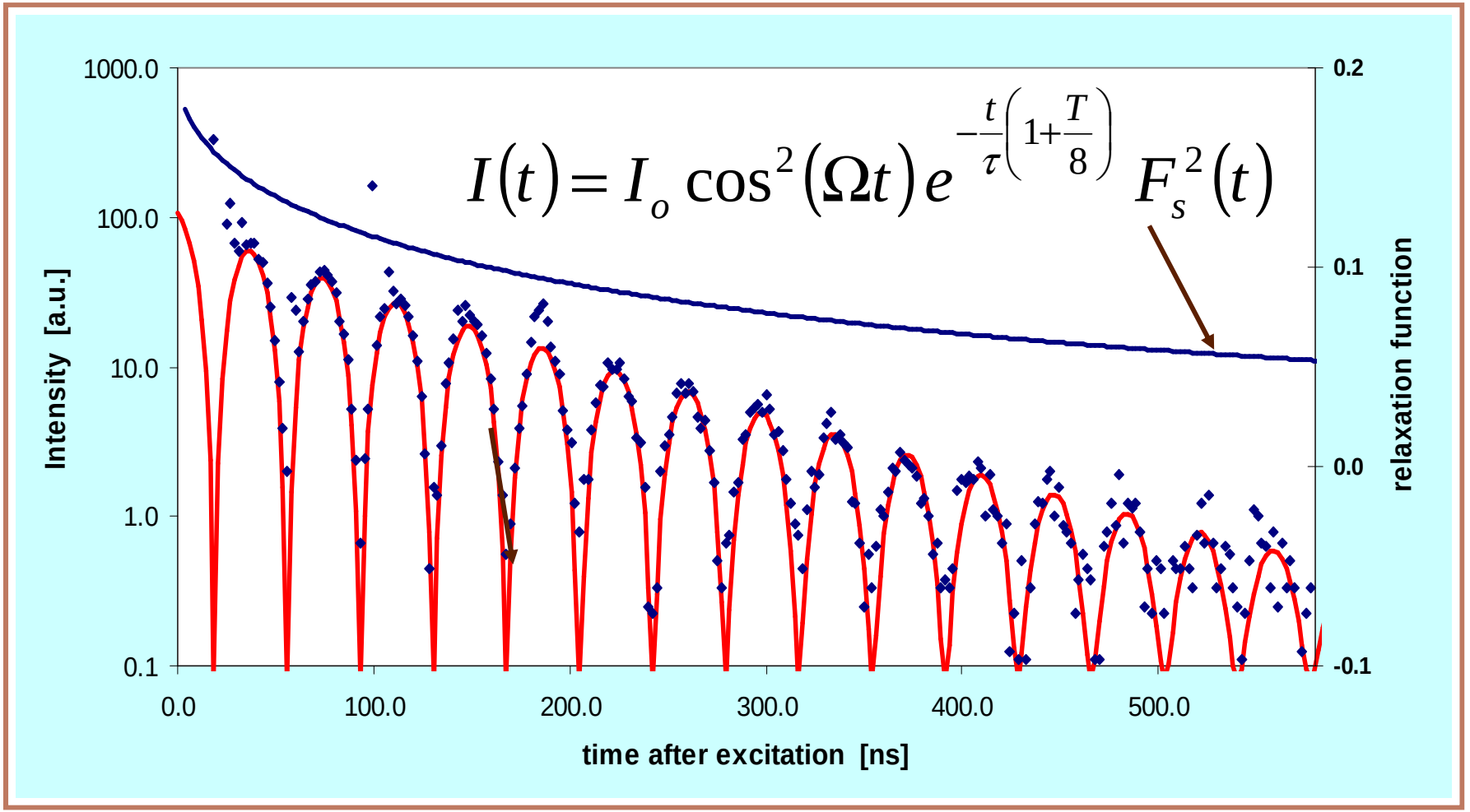

Butyl phthalate / ferrocene

Exact treatment of QNFS: I. Sergueev, HF,.. PRB 2003

Non ergodicity parameter

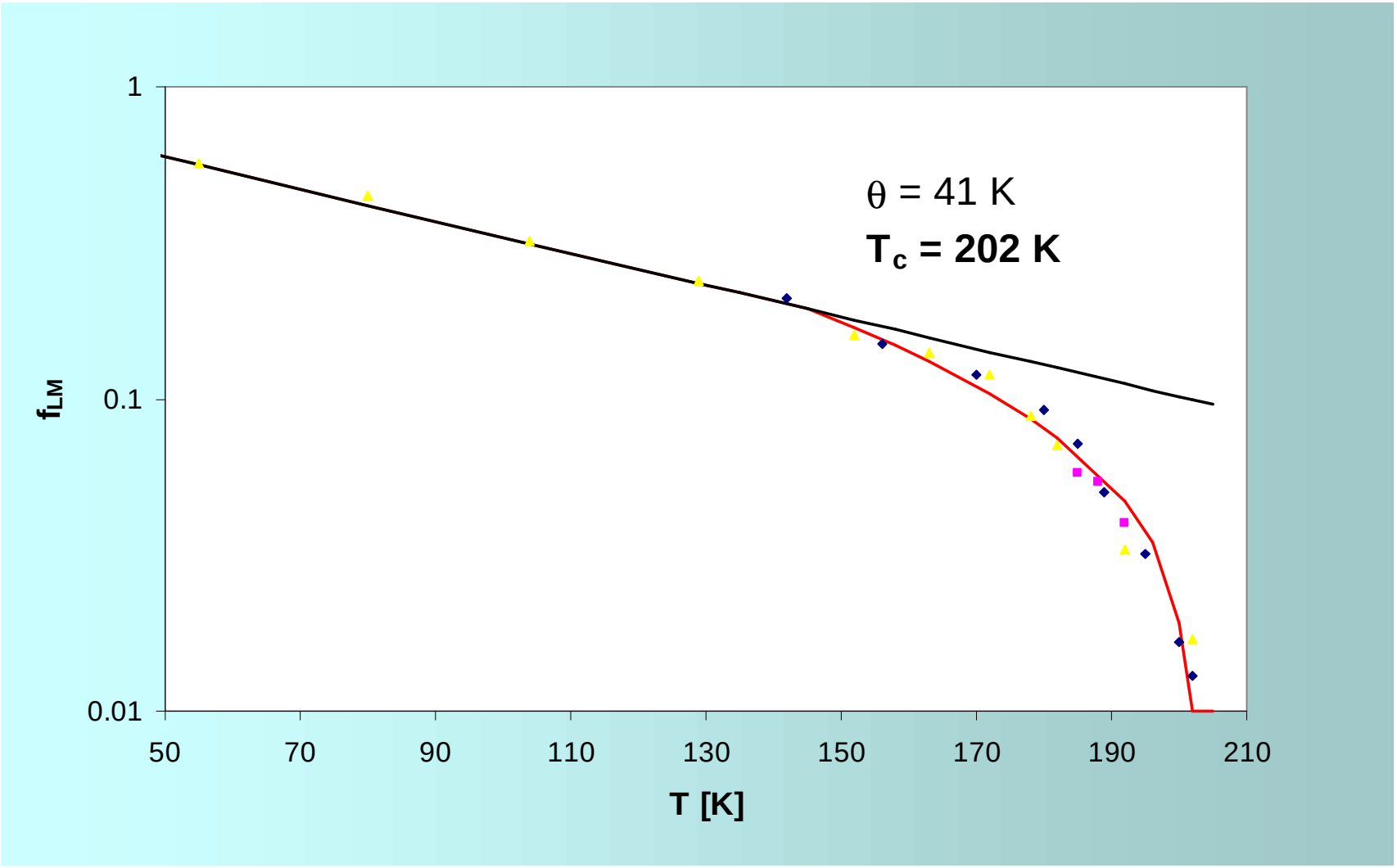

Square-root behaviour as predicted by mode-coupling theory

Stretching exponent $\beta = 0.48$, independent of T

Neutron scattering results

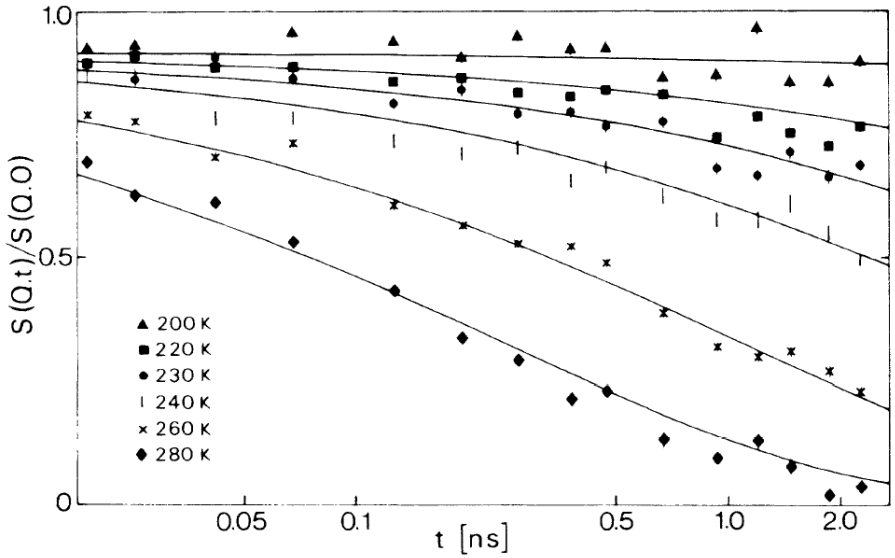

Masterplot

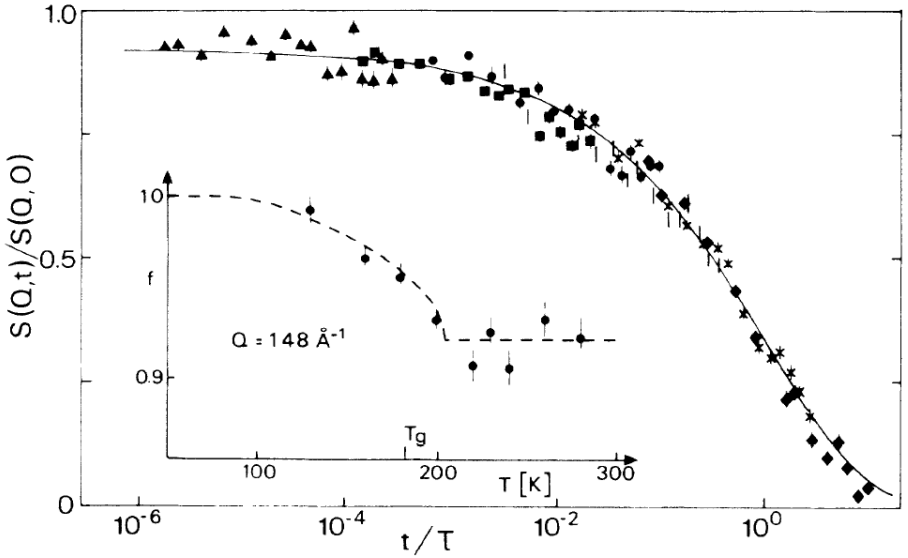

J. Wuttke et al, Physica B (1997)

Structure determination of amorphous materials

X-ray diffraction using high energy photons

+ high penetration depths (mm-cm)
+ relatively fast, suitable for in-situ studies
- less sensitive to elements
- ASF depend on Q

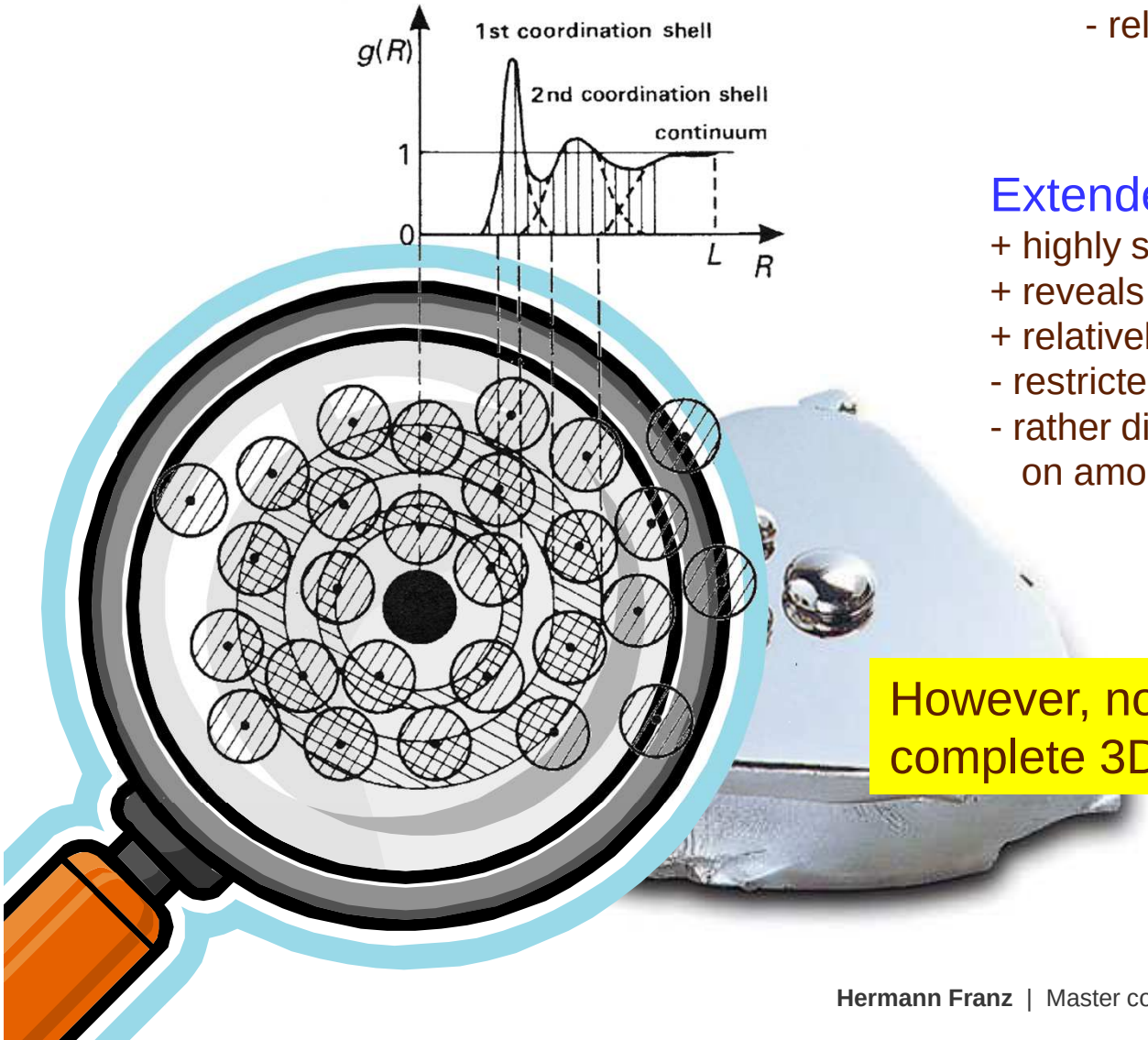

Neutron diffraction

+ sensitive to different isotopes
+ ASF do not depend on Q
+ probes magnetic state of matter
- large sample volumes
- relatively slow, not suitable for in-situ studies

Extended X-ray Absorption Spectroscopy

+ highly sensitive to elements
+ reveals local atomic configuration
+ relatively fast, suitable for in-situ studies
- restricted sample size, geometry
- rather difficult to quantitatively analyze data on amorphous samples

However, none of these techniques gives a complete 3D image of amorphous structure ☹

In-situ tensile experiments using high-energy XRD

BW5 is dedicated to X-ray scattering experiments using high-energy photons (**60 - 150 keV**).

The **large penetration depth** at these energies of typically **sereral mm to cm** allows the investigation of bulk materials and complex sample environments.

The experimental station is equipped with a triple axis diffractometer and an **image plate** camera.

Parameters:

- **wavelength λ = 0.12398 Å (100 keV)**
- **crossection of collimated beam 1mm²**
- **exposure time 10 s**
- **XRD in transmission mode**
- **2D ma345 image plate detector used in symetric mode**

Absorption scan.

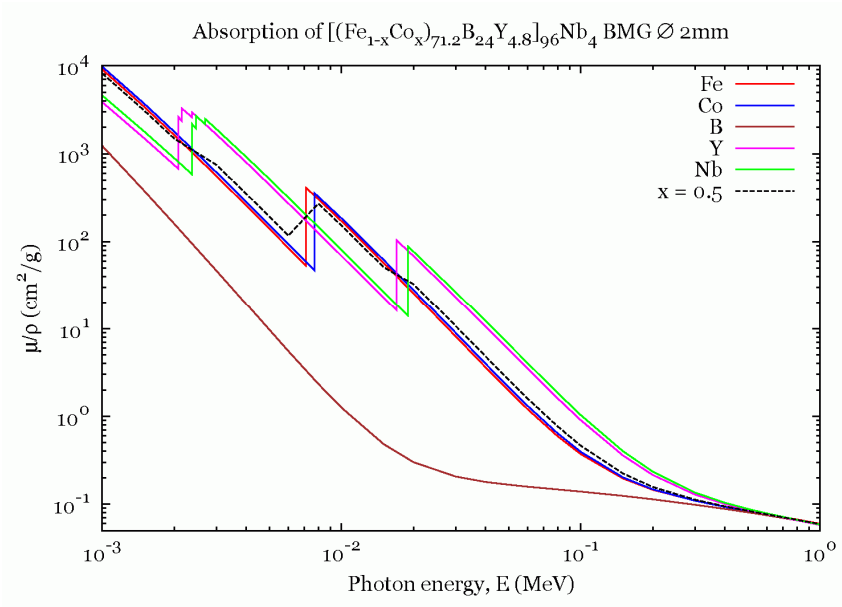

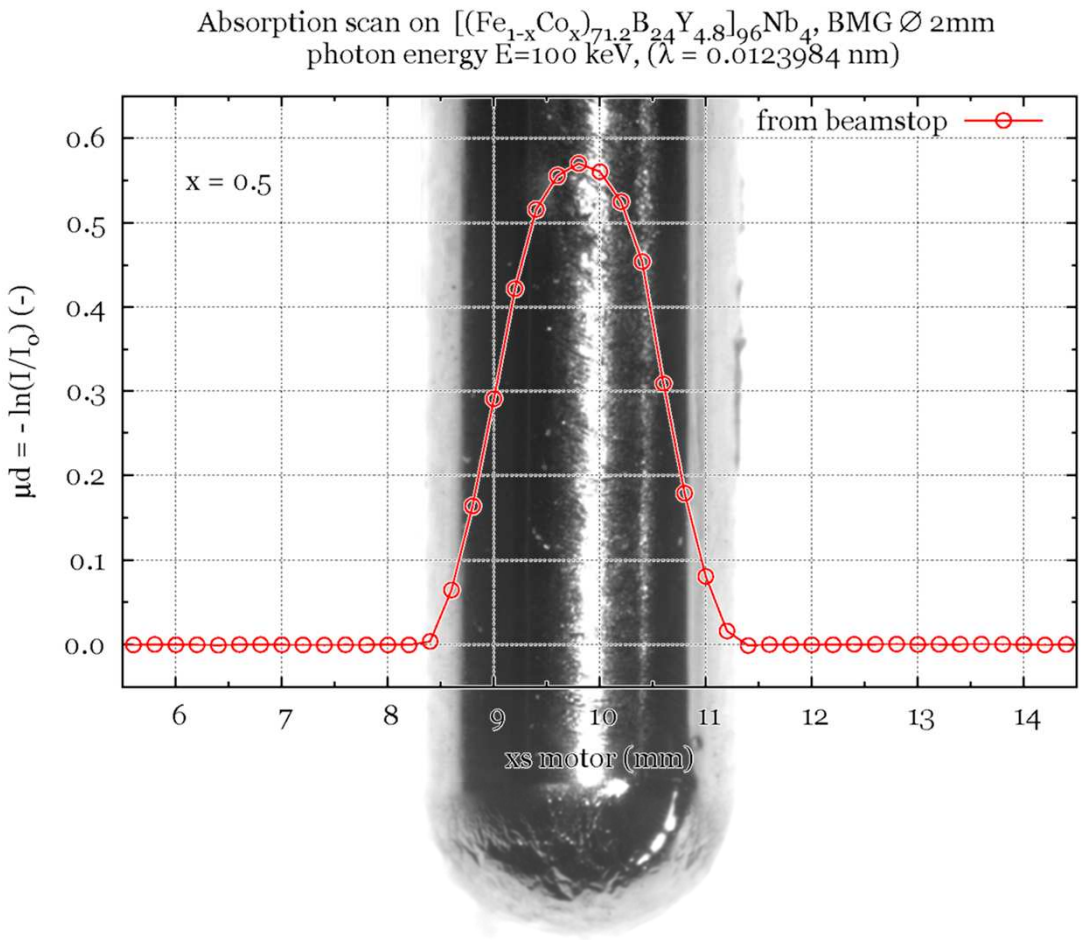

$$I = I_0 e^{-\mu d}$$

I_o represents incident intensity

I is the transmitted intensity

μ is the absorption coefficient

d is the sample thickness

M. Stoica et al, *Journal of Applied Physics* 109 (2011) 054901

Calculation of structure factor.

The measured X-ray diffraction intensity may be expressed [10] by

$$I^{mea}(Q) = PA[N(I^{coh}_{eu} + I^{inc}_{eu} + I^{mul}_{eu})] \tag{5.1}$$

where P is the polarization factor, A the absorption factor, N normalization constant, and $I^{coh}_{eu}, I^{inc}_{eu}, I^{mul}_{eu}$ are the coherent, incoherent(Compton), and multiple scattering intensities, respectively, in electron units. We can define the structure function($S(Q)$) in the following form.

$$S(Q) = [I^{coh}_{eu} - (\langle f^2 \rangle - \langle f \rangle^2)]/\langle f \rangle^2 \tag{5.2}$$

where $\langle f \rangle$ is the sample average scattering factor. Therefore to get a structure function, we have to do the following corrections [11] step by step on raw data.

0) Dead-time correction

1) Multiple scattering correction

2) Polarization correction

3) Absorption correction

4) Normalization

5) Compton scattering correction

6) Laue diffuse correction

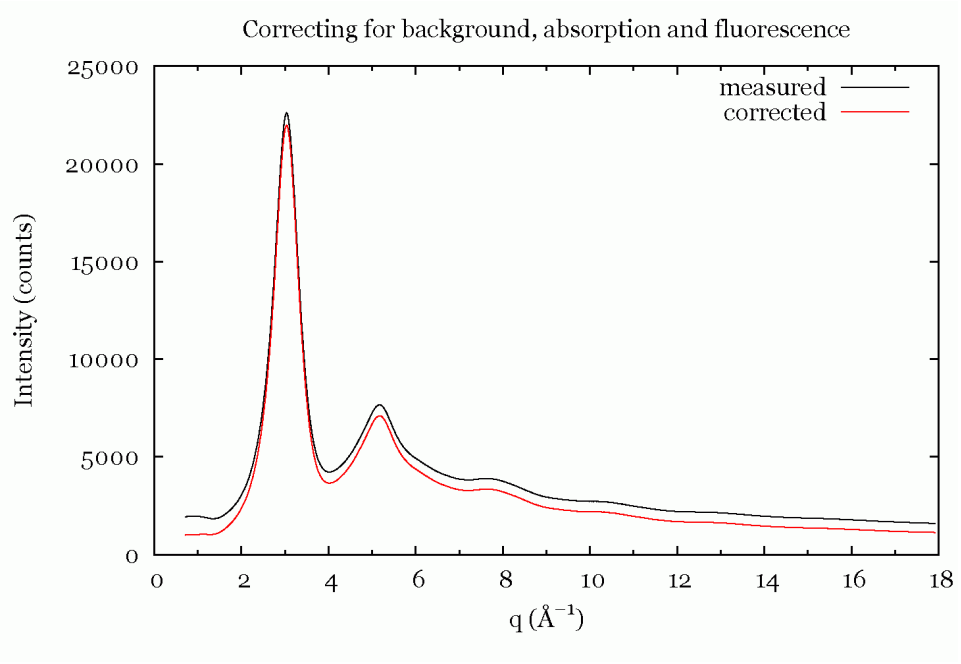

[10] Y. Waseda. *The structure of non-crystalline materials.* McGraw-Hill, New York, 1980.

[11] C. N. J. Wagner, J. Non-Cryst. Solid **31**, 1, 1978

Compton scattering.

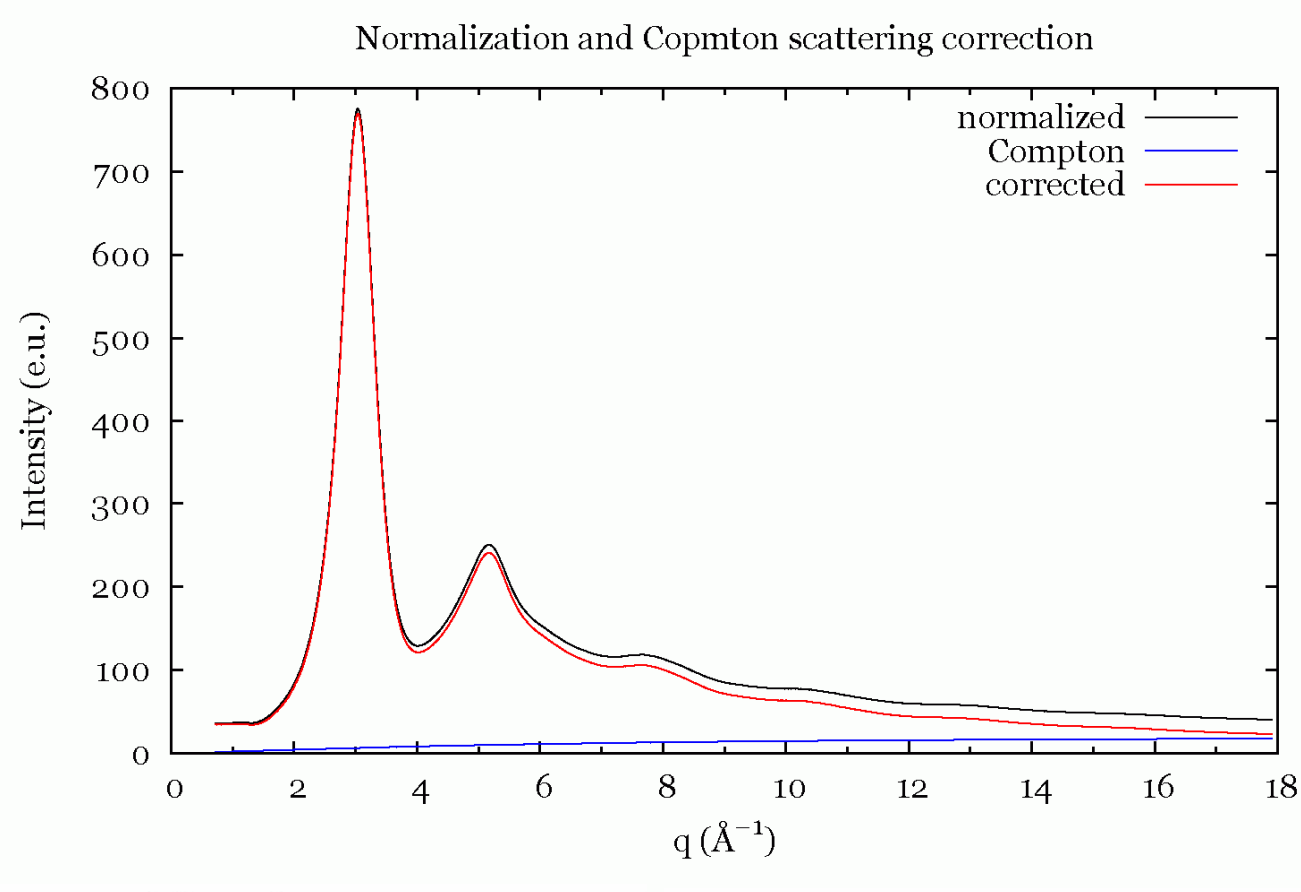

(*b*) *The incoherently diffracted intensity per atom,* $I_a^{\text{incoh}}(Q)$

$$I_a^{\text{incoh}}(Q) = \left(\frac{\lambda}{\lambda'}\right)^2 \sum_{j=1}^{n} c_j Z_j \frac{(b_j Q)^{a_j}}{1+(b_j Q)^{a_j}} \qquad (A2)$$

with n the number of atomic species, Z_j the atomic number of species j, and a_j and b_j semi-empirical expressions given by

$$a_j = 2{\cdot}6917\, Z_j^{-1} + 1{\cdot}2450 \qquad (A3)$$

$$b_j = 1{\cdot}1870\, Z_j^{-1} + 0{\cdot}1075 + 0{\cdot}00436\, Z_j - (0{\cdot}01543\, Z_j)^2 + (0{\cdot}01422\, Z_j)^3. \qquad (A4)$$

J. Appl. Cryst. (1984). **17**, 61–76

Laue diffuse scattering.

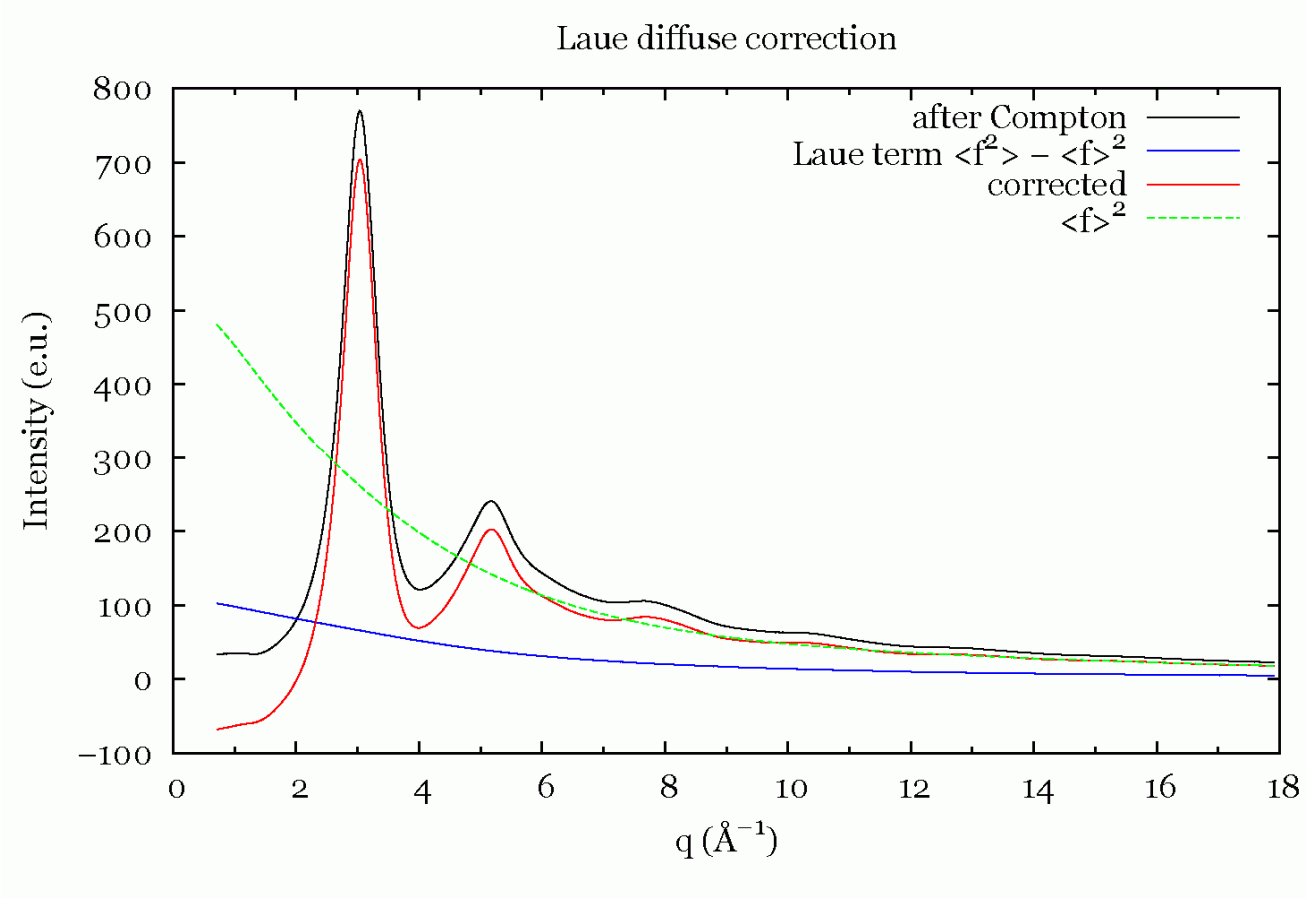

(*a*) *The complex scattering power for atomic species j*

$$f_j(Q) = f_j^0(Q) + f'_j(\lambda) + if''_j(\lambda), \qquad (A1)$$

where f^0 is calculated using the analytical expressions given in *International Tables for X-ray Crystallography* (1974), and f' and f'' are taken from Cromer & Liberman (1970).

J. Appl. Cryst. (1984). **17**, 61–76

$$\langle f^2 \rangle = \left[\sum_{i=1}^{n} c_i f_i^2(q) \right]$$

$$\langle f \rangle^2 = \left[\sum_{i=1}^{n} c_i f_i(q) \right]^2$$

Structure factor.

- Measured intensities corrected for absorption, polarization, fluorescence, multiple scattering, Compton scattering
- Proper normalization based on weighted atomic scattering factors (Faber-Zimman formalism)

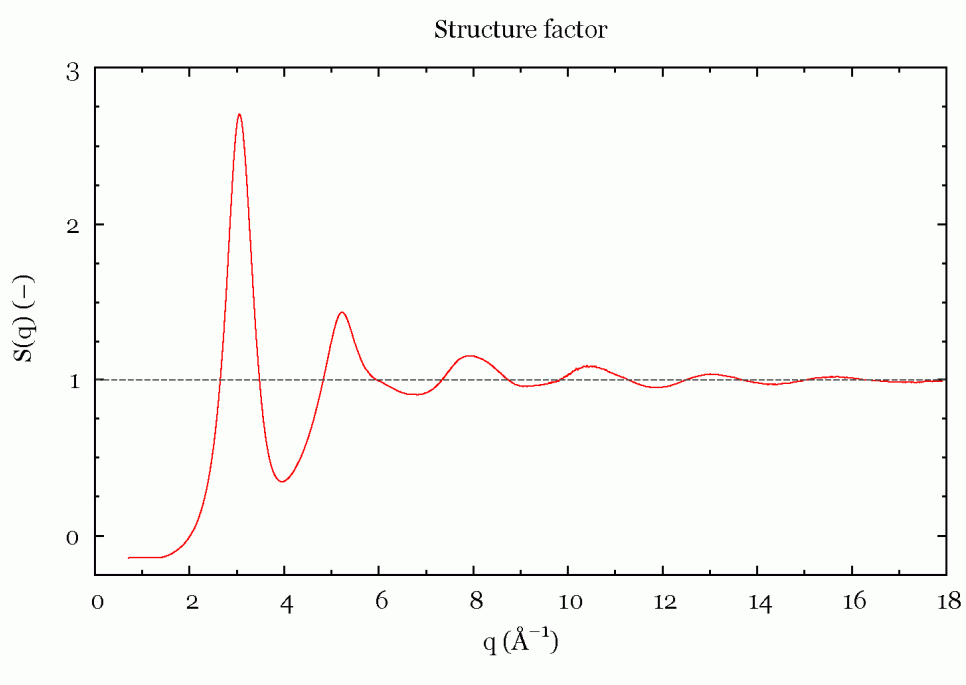

$$S(q) = 1 + \frac{I^{coh}(q) - \langle f^2 \rangle}{\langle f \rangle^2} \qquad (1)$$

where $\langle f \rangle = \sum_{i=1}^{n} c_i f_i(q)$ and $\langle f^2 \rangle = \sum_{i=1}^{n} c_i f_i^2(q)$, in which c_i corresponds to the atomic fraction of the component i having X-ray atomic scattering factor $f_i(q)$. The reduced pair distribution function, $G(r)$, can be obtained through a sine Fourier transformation

$$G(r) = \frac{2}{\pi} \int_0^{\infty} q[S(q) - 1] \sin(qr)\, \mathrm{d}q. \qquad (2)$$

Pair Distribution Function.

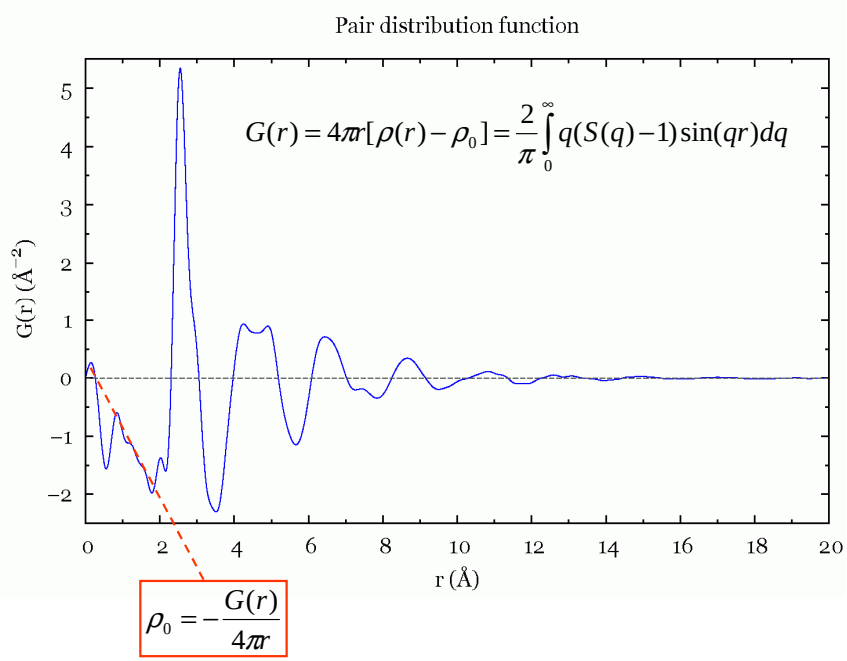

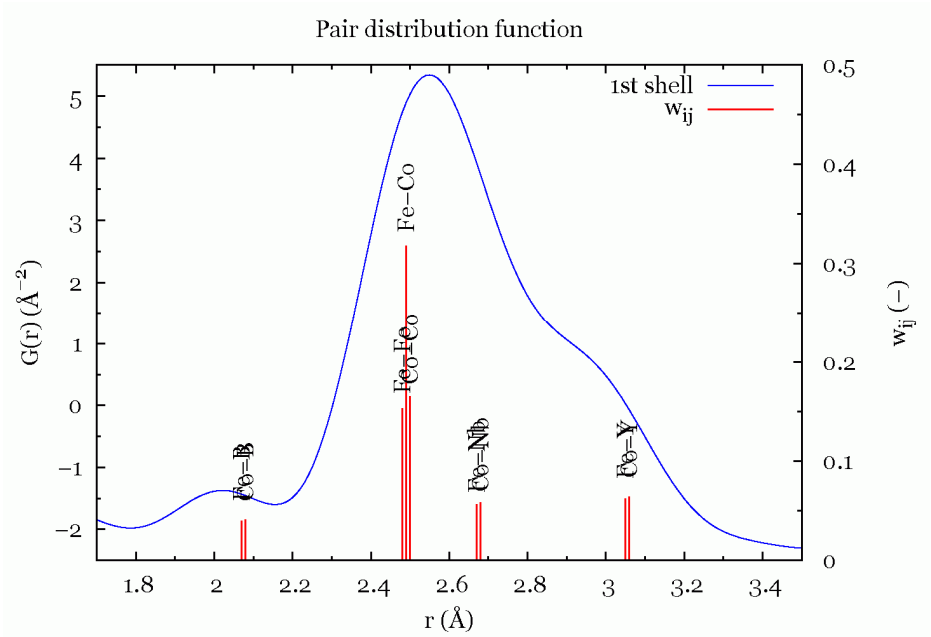

$$g(r) = \frac{\rho(r)}{\rho_0} = \frac{G(r)}{4\pi\rho_0 r} + 1$$

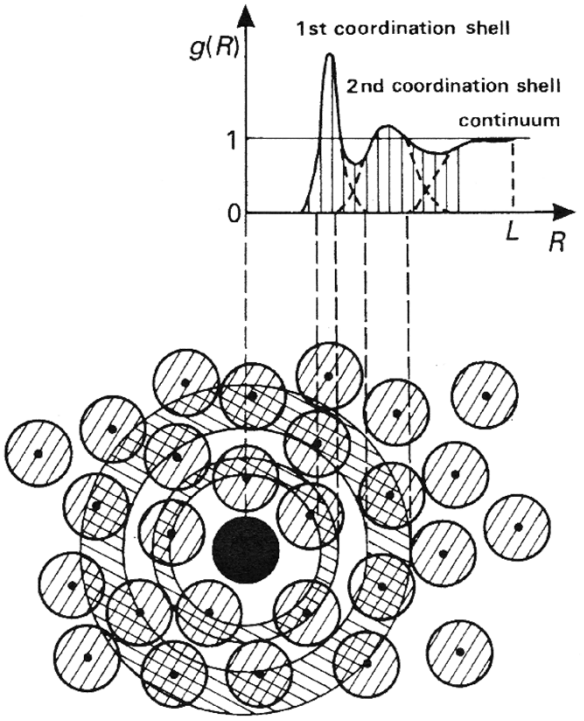

g(r) describes how the density of surrounding atoms varies as a function of the distance from a distinguished atom.

Coordination number.

$$CN = \int_{r_1}^{r_2} RDF(r)dr = \int_{r_1}^{r_2} \left[4\pi\rho_0 r^2 + rG(r)\right]dr$$

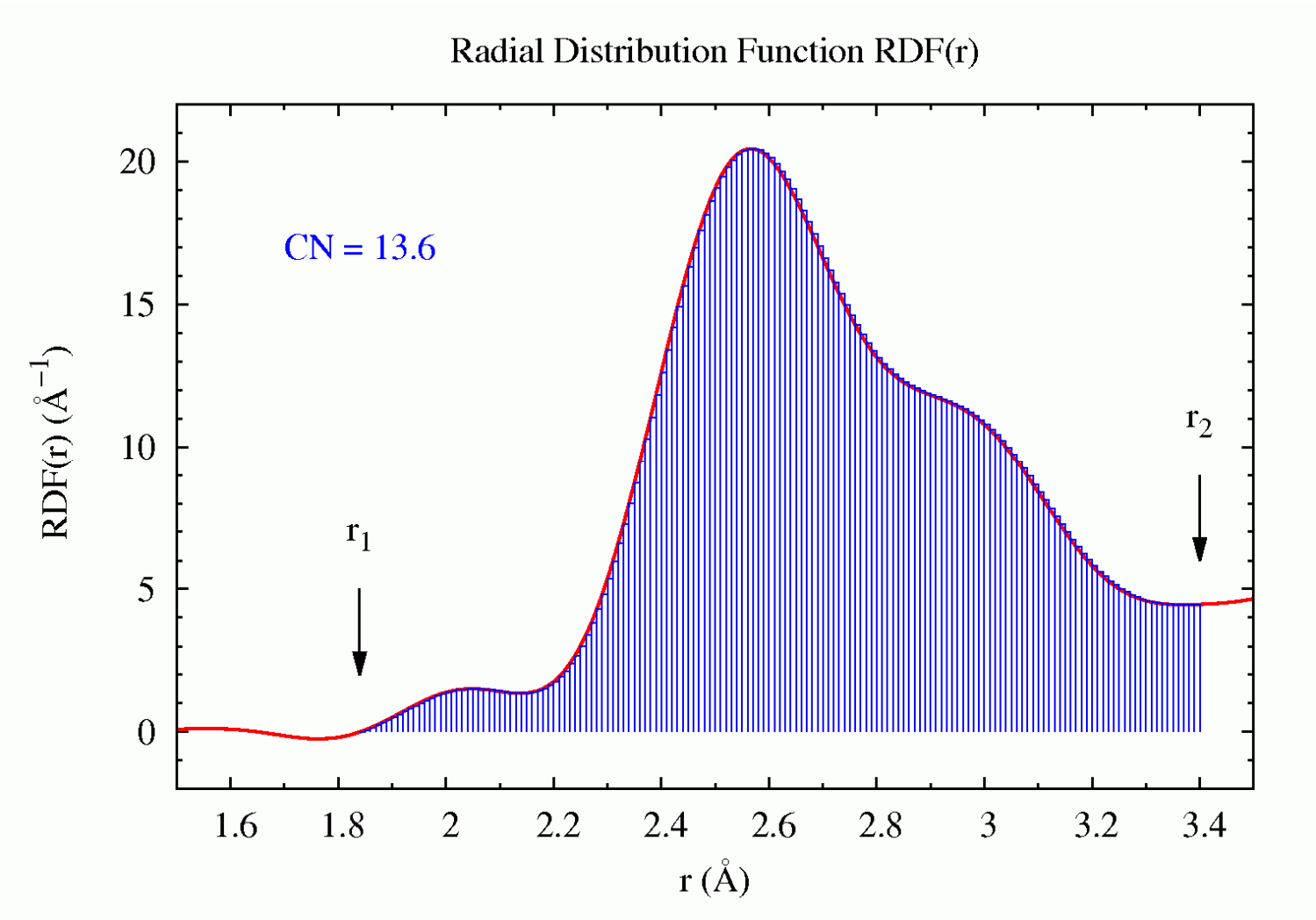

Resolution in real space.

- Collecting diffracted photons up to high q values significantly improves resolutions of pair distribution function

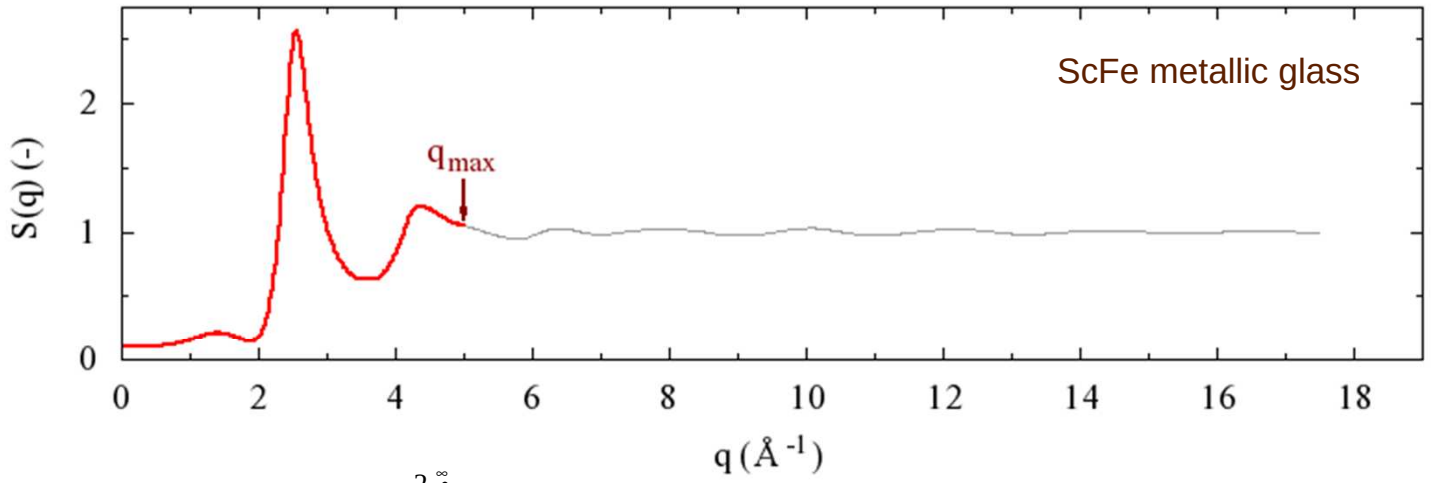

$$G(r) = 4\pi r[\rho(r) - \rho_0] = \frac{2}{\pi}\int_0^\infty q(S(q)-1)\sin(qr)dq$$

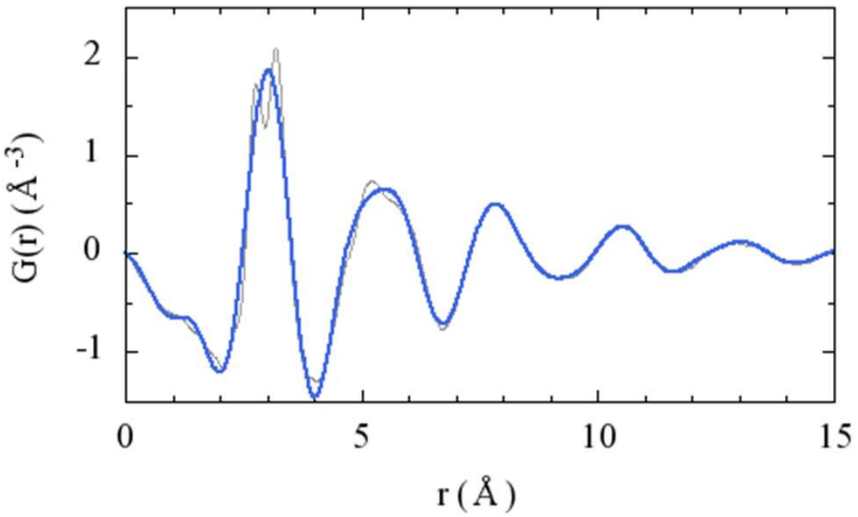

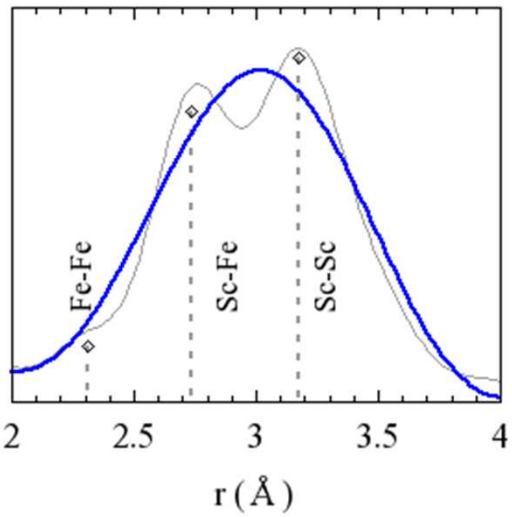

Summary.

1) Measure diffracted photons up to high q-range

$$q_{\max} = \frac{4\pi}{\lambda}\sin\left[\frac{1}{2}arctg\left(\frac{R}{SD}\right)\right]$$

2) Perform corrections and calculate structure factor S(q)

$$S(q) = 1 + \frac{I_{e.u}^{coh} - \langle f^2 \rangle}{\langle f \rangle^2} \qquad \langle f^2 \rangle = \left[\sum_{i=1}^{n} c_i f_i^2(q)\right] \qquad \langle f \rangle^2 = \left[\sum_{i=1}^{n} c_i f_i(q)\right]^2$$

3) Fourier transformation of S(q) one obtains Pair Distribution Function G(r)

$$G(r) = 4\pi r[\rho(r) - \rho_0] = \frac{2}{\pi}\int_0^{\infty} q(S(q)-1)\sin(qr)dq$$

4) Determine mean atomic density from G(r) on low r-range

$$G(r) = -4\pi r\rho_0$$

4) Calculate Coordination Number (CN) from Radial Distribution Function RDF(r)

$$CN = \int_{r_1}^{r_2} RDF(r)dr = \int_{r_1}^{r_2}\left[4\pi\rho_0 r^2 + rG(r)\right]dr$$

In-situ tensile experiments

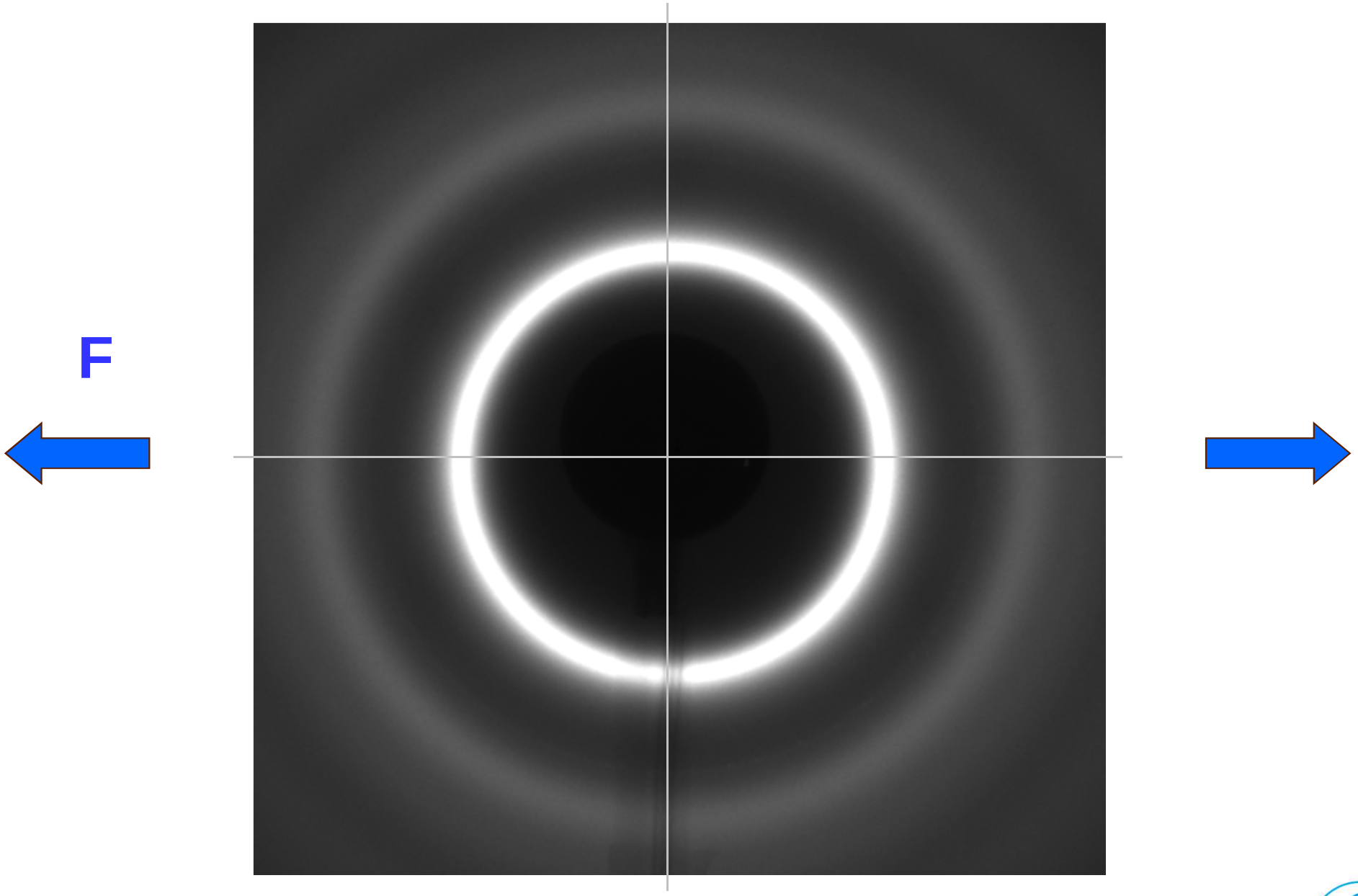

Courtesy J. Bednarcik

Determination of deformation state by XRD

The symmetric circular diffraction pattern is characterized with respect to the polar coordinates (*s*, η). By dividing the η-range of 0 to 2π into 36 segments, one obtains symmetrized intensity distributions

$$I'_i(Q,\eta_i) = \int_{\eta_i-\pi/36}^{\eta_i+\pi/36} [I(Q,\eta) + I(Q,\eta+\pi)]\, d\eta$$

with i = 1…18, where the wave-vector transfer $Q = Q(s)$ is defined by

$$Q(s) = \frac{4\pi}{\lambda} \sin\left(\frac{1}{2} arctg\left(\frac{s}{D}\right)\right)$$

in which λ denotes the wavelength, D refers to the sample-to-detector distance and s represents the distance from the origin of the polar coordinate system.

The relative change of the position of the principal peak upon applying an external stress defines the strain

$$\varepsilon_i(\eta_i,\sigma) = \frac{q(\eta_i,0) - q(\eta_i,\sigma)}{q(\eta_i,\sigma)}$$

H. F. Poulsen et al., *Nat. Mater.* **4** 33-35 (2005)

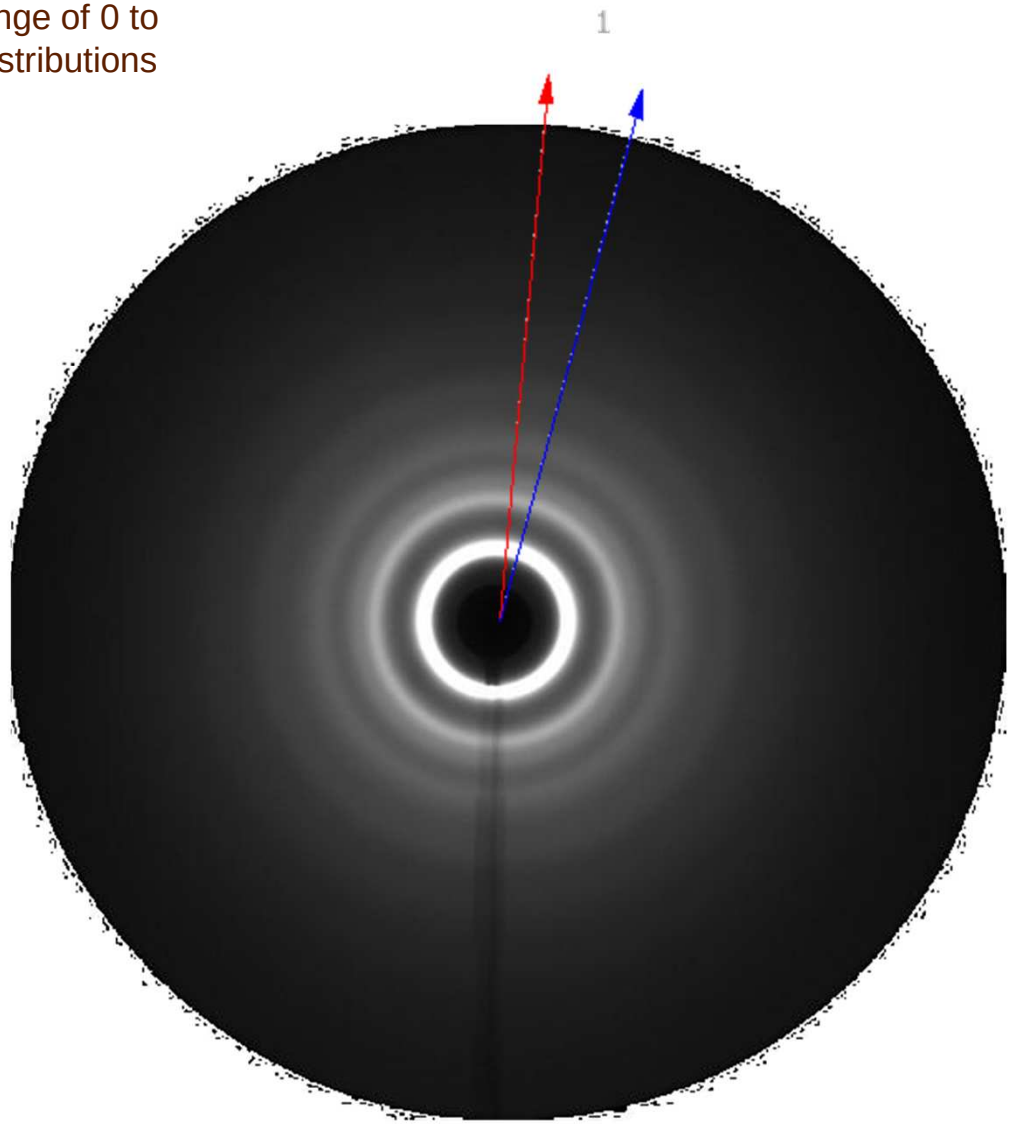

Determination of tensor components

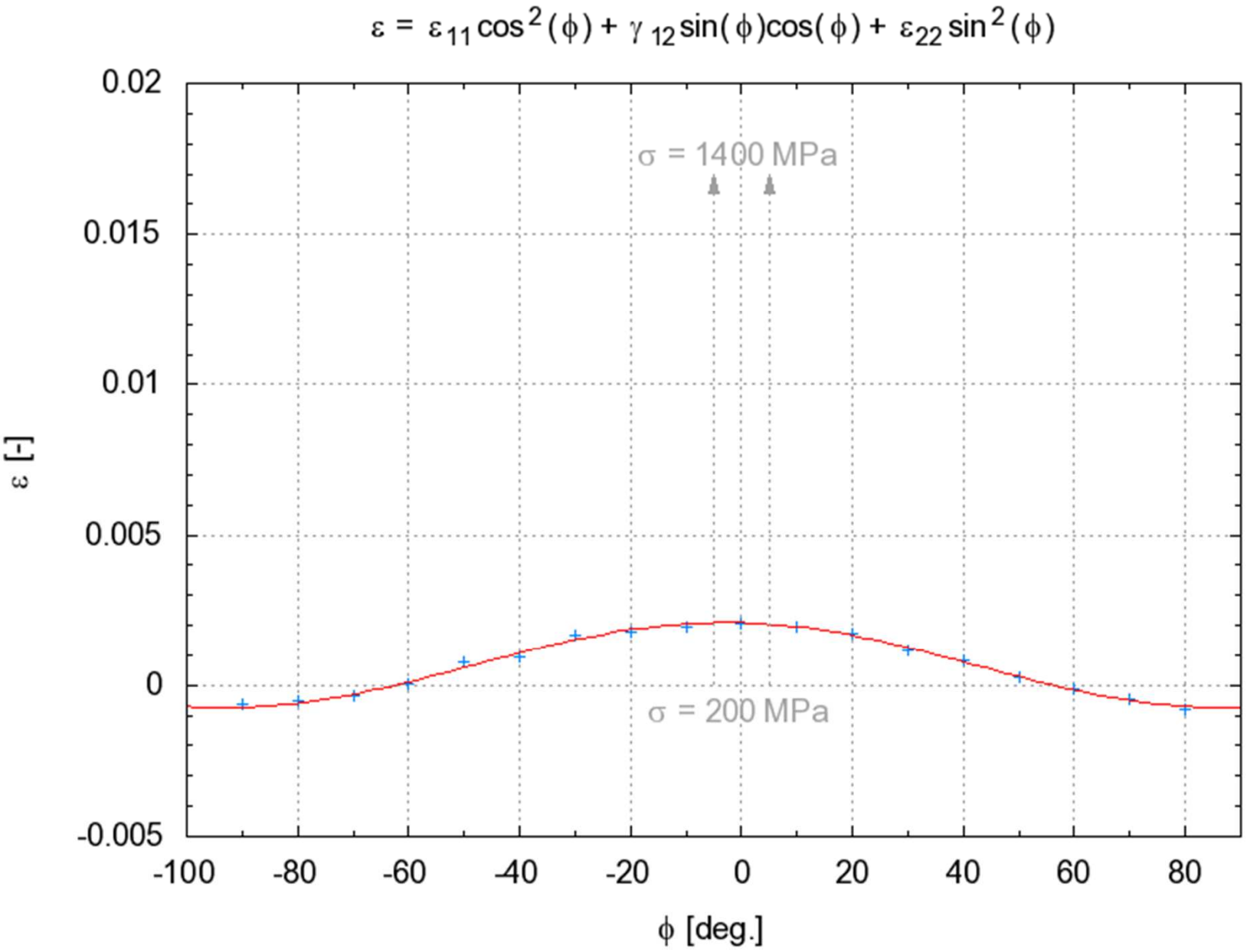

Analysis in reciprocal space

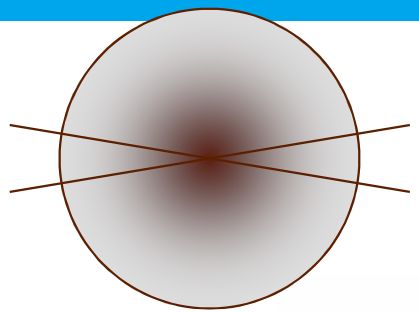

$$S(Q) = 1 + \frac{I_e(Q) - \left[\sum_{i=1}^{n} c_i f_i^2(Q)\right]}{\left[\sum_{i=1}^{n} c_i f_i(Q)\right]^2}$$

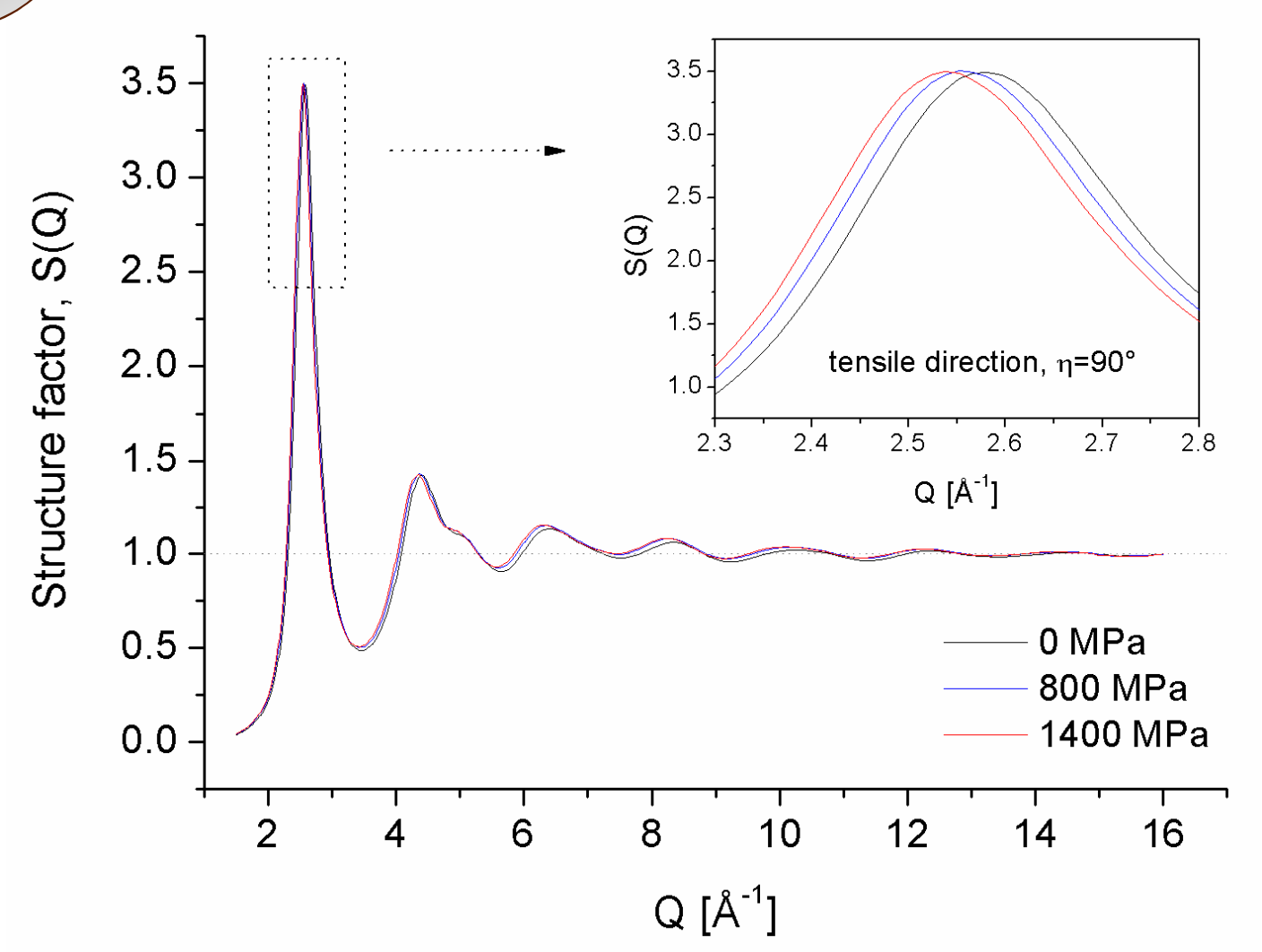

Stress-strain curves

Poly-crystalline metal

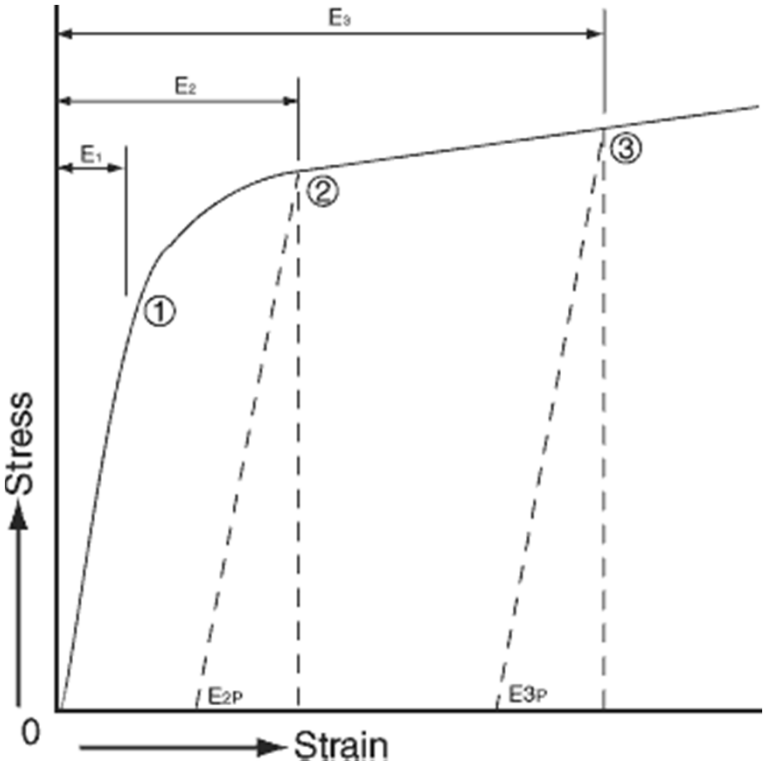

La based metallic glass

Only elastic strain !!!

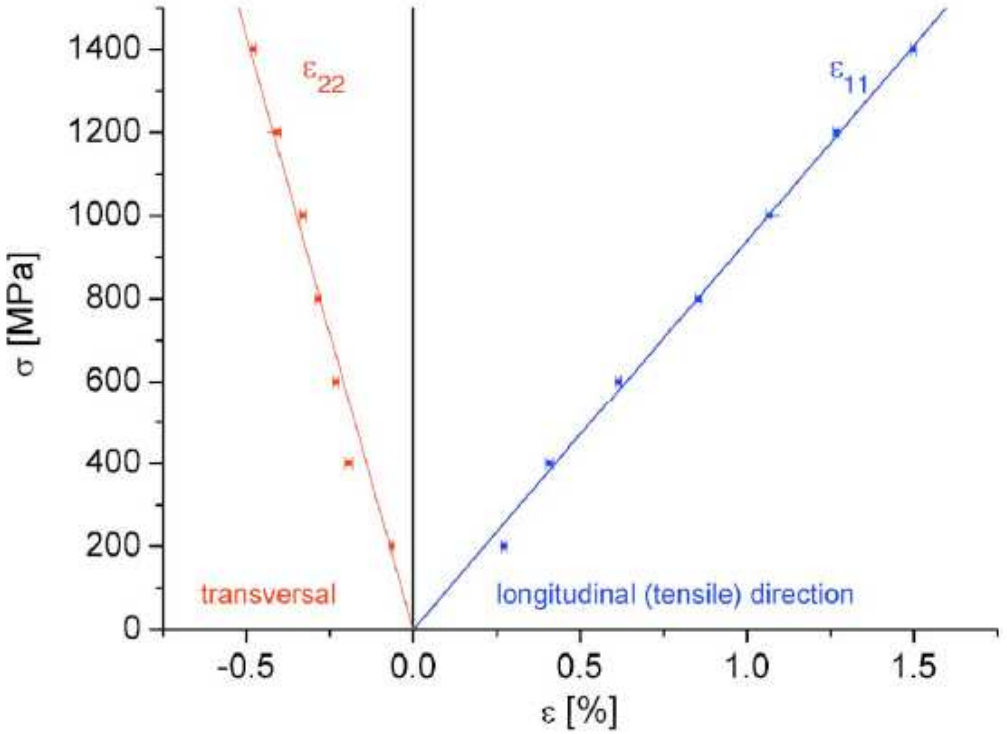

Tensile deformation at elevated temperatures.

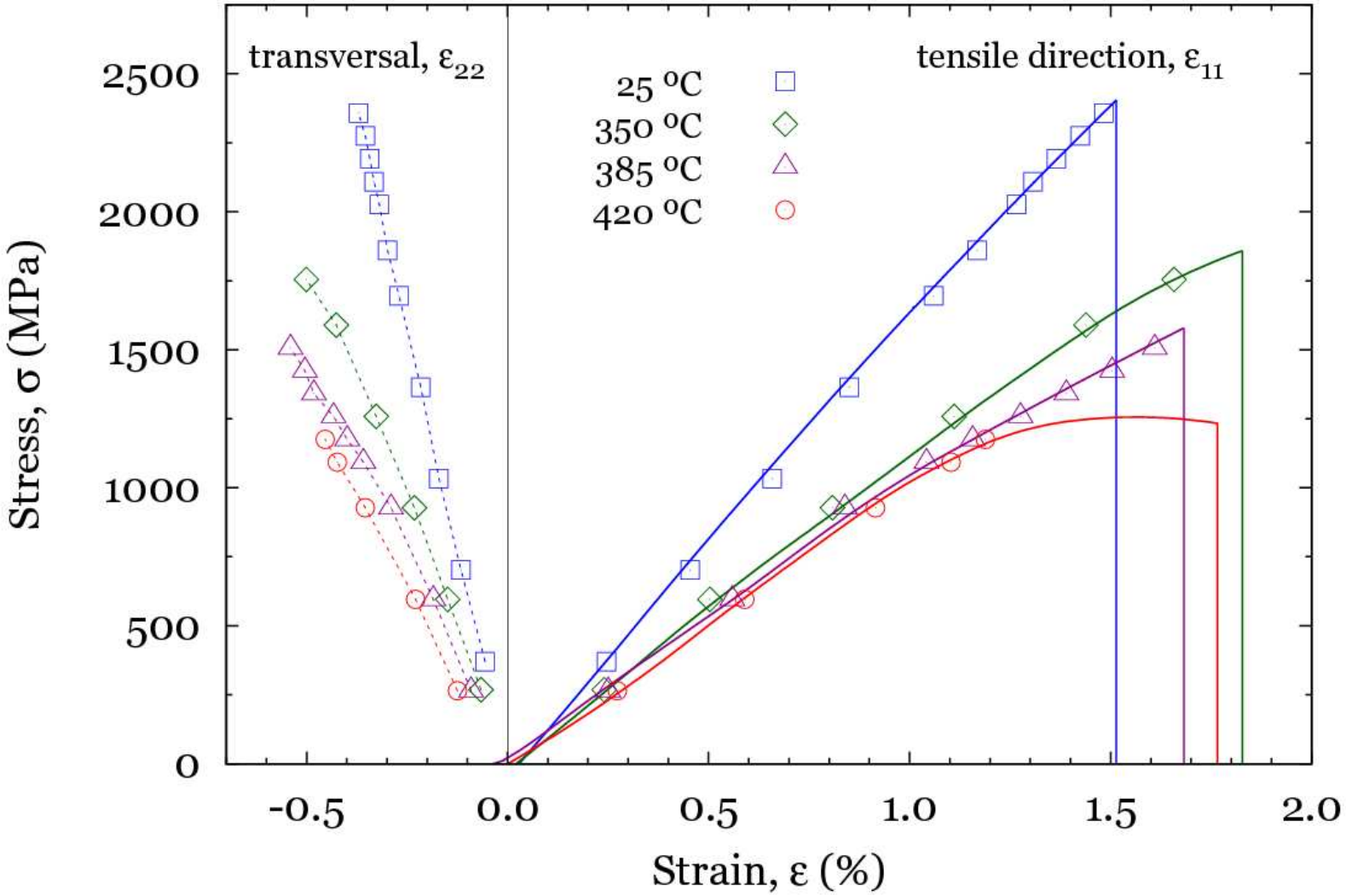

J. Bednarcik et al., J. Aloy Comp,
DOI 10.1016/j.jallcom.2010.12.007

Relaxation phenomena and glass transition

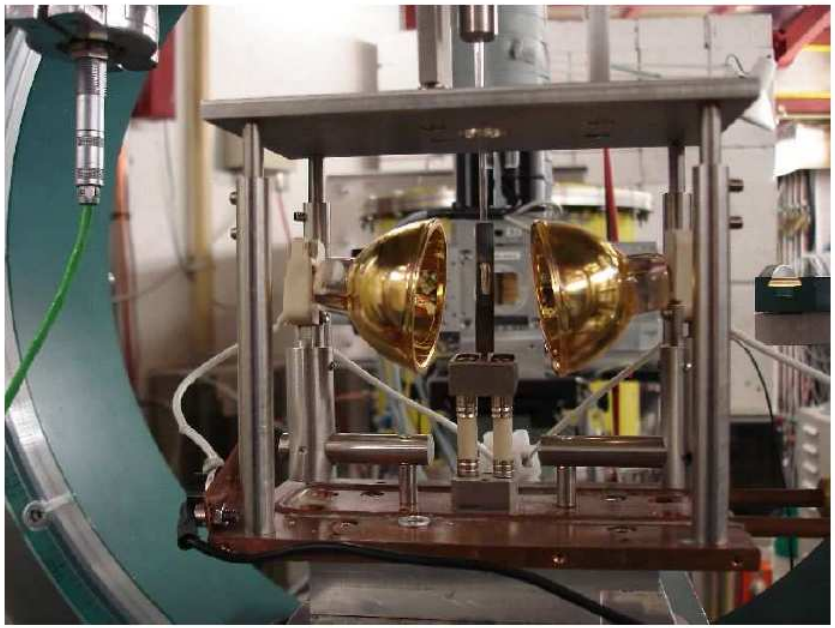

Figure 1: Detailed view showing infrared lamp furnace. Black tube sitting between two lamps supports capillary with the sample and serves as a heat condenser.

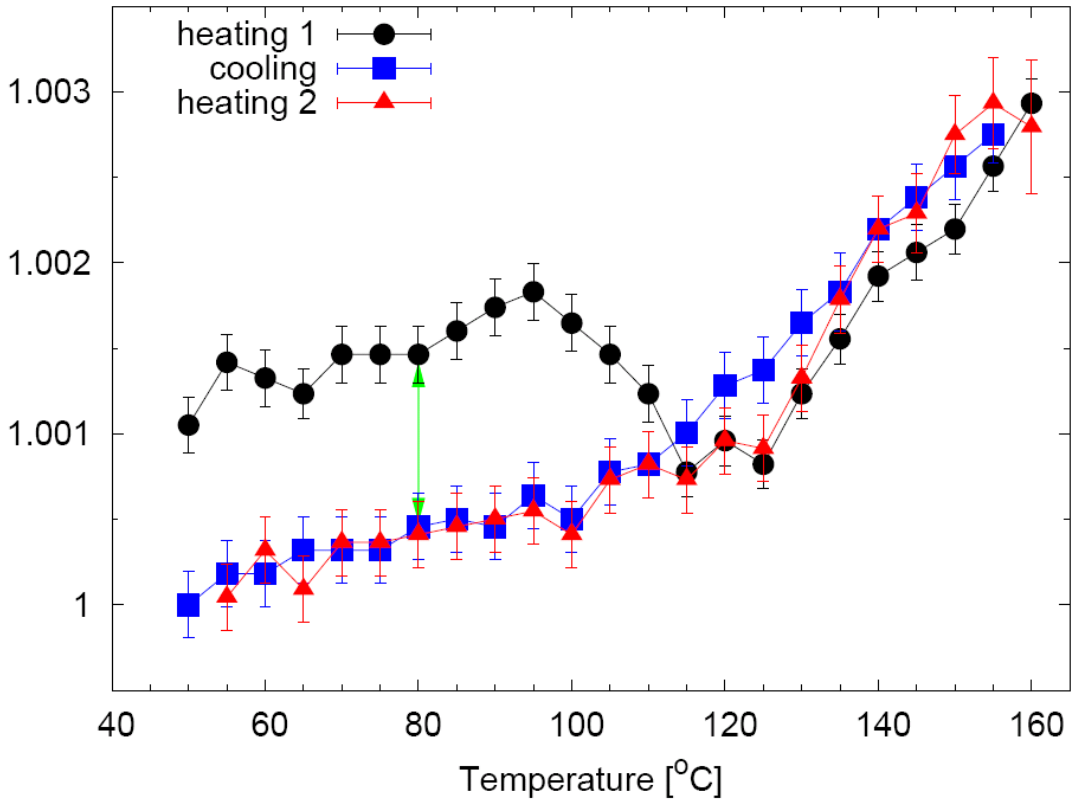

Relaxation phenomena and glass transition

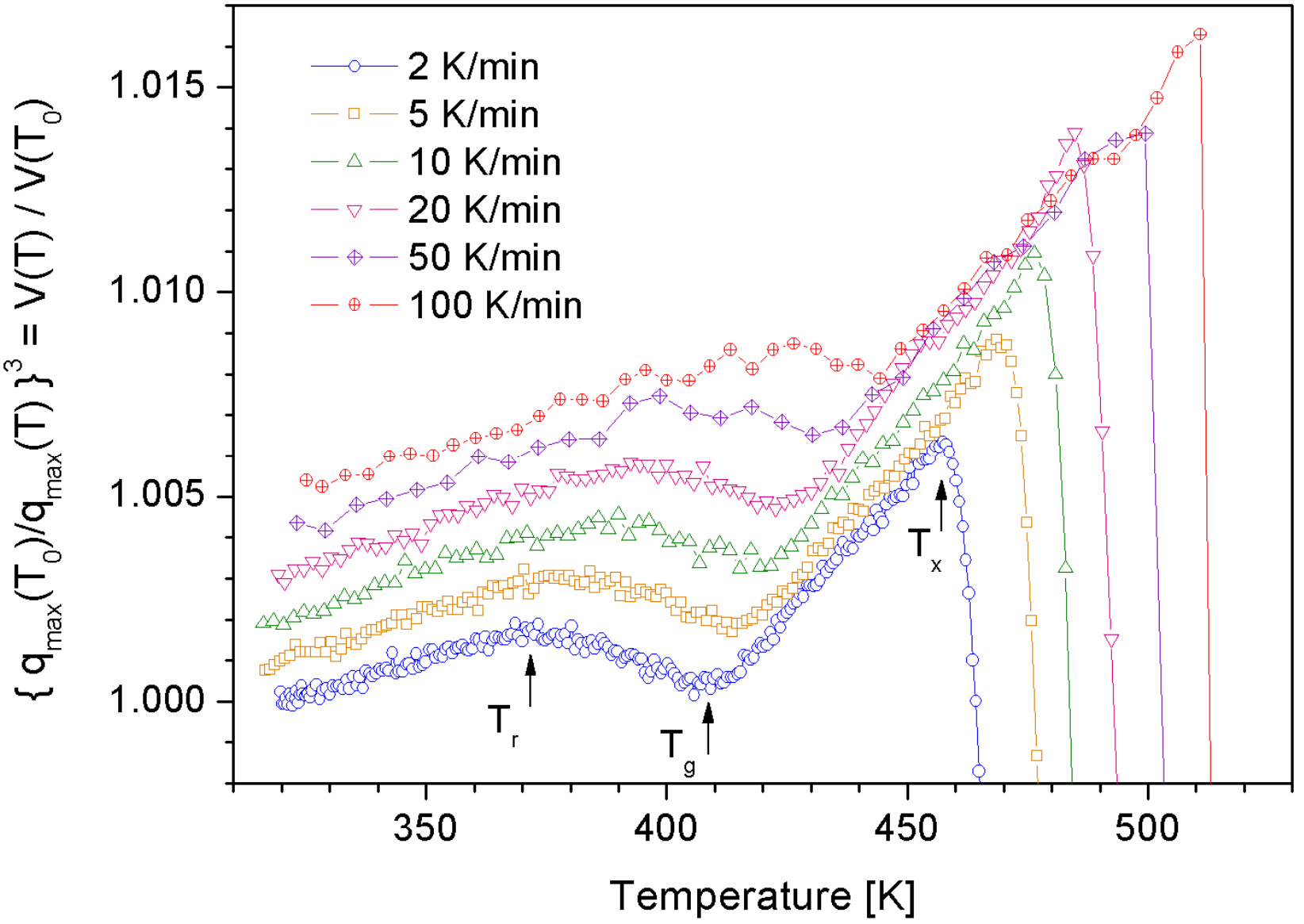

Structure by X-rays - temperature dependence II

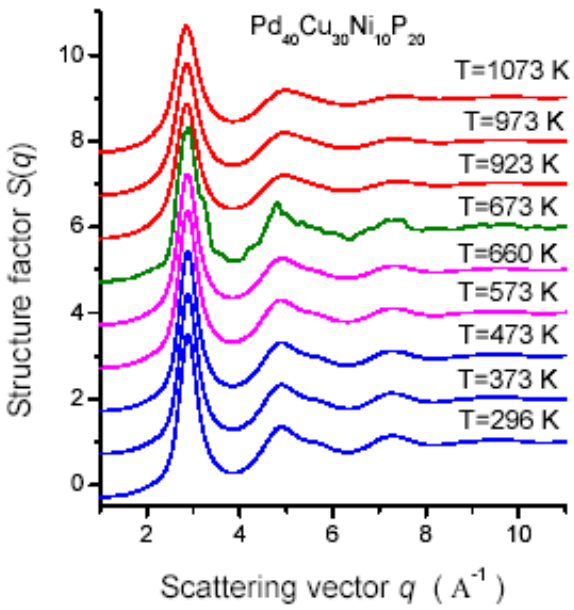

Fig.1:Structure factor $S_T(q)$ of $Pd_{40}Cu_{30}Ni_{10}P_{20}$ at different temperatures

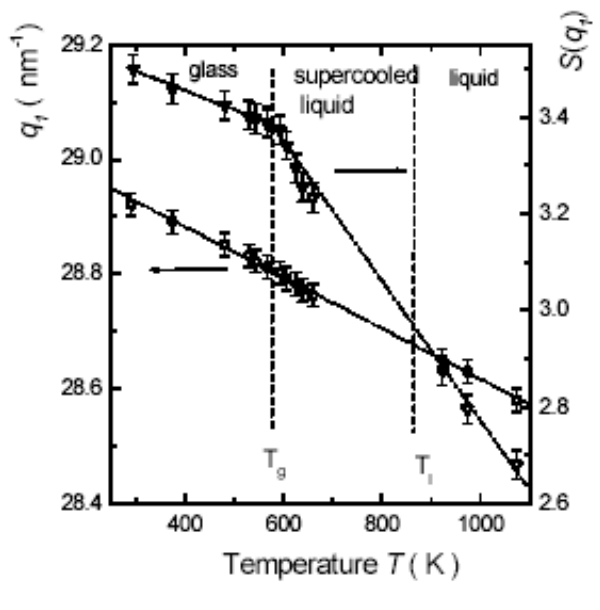

Fig.2: Position q_1 and height $S(q_1)$ of the first maximum of the structure factor $S_T(q)$ vs temperature

N. Mattern et al
APL 2003

Below T_g: harmonic change, described by Debye behavior
At T_g: Transition to lower Debye-temperature
+ structural changes

Structure vs. macroscopic properties

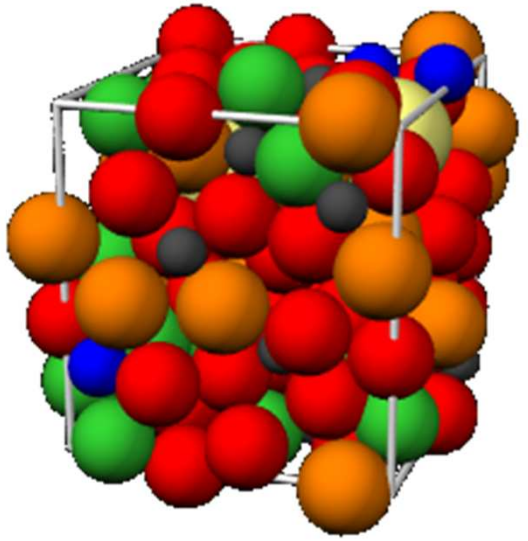

Understanding relation between the structure and macroscopic properties is important for improving performance of existing and crucial for designing novel materials